J|A|C|S
ARTICLES
Published on Web 03/05/2004

The Role of Large Conformational Changes in Efficient Ultrafast Internal Conversion: Deviations from the Energy Gap Law

Henk Fidder,*,† Matteo Rini,‡ and Erik T. J. Nibbering‡

Contribution from the Department of Physical Chemistry, Uppsala University, P.O. Box 579, S-751 23 Uppsala, Sweden, and Max-Born-Institut für Nichtlineare Optik und Kurzzeitspektroskopie, Max Born Strasse 2A, D-12489, Berlin, Germany

Received September 26, 2003; E-mail: henk.fidder@fki.uu.se

Abstract: Conversion of electronic excitation energy into vibrational energy was investigated for photochromic spiropyran molecules, using femtosecond UV−mid-IR pump−probe spectroscopy. We observe a weaker energy gap dependence than demanded by the "energy gap law". We demonstrate that large conformational changes accompanying the optical excitation can explain the observed time scale and energy gap dependence of ultrafast $S_1 \rightarrow S_0$ internal conversion processes. The possibility of dramatic deviations from standard energy gap law behavior is predicted. We conclude that controlling molecular conformations by rigid environments can have a substantial impact on photophysical and (bio)chemical processes.

Introduction

Internal conversion (IC) is a process through which electronic excitation energy is converted into vibrational excitation energy[1,2] (see Figure 1). Internal conversion plays a crucial role in many photoinduced and biological processes. For instance, it enables photostabilization of polymers[3] and expands the energy harvesting range in photosynthesis with the help of carotenoids.[4] Efficient internal conversion also occurs in DNA and RNA nucleosides[5] and is believed to be an important factor in increasing genomic stability and preventing photodamage, and thus suppresses the possibility of skin cancer.

Usually IC is ultrafast from highly excited states to the lowest electronic excited state,[1,2,4,6] that is, $S_n \rightarrow S_1$. Relaxation from the lowest electronic excited state, on the other hand, tends to be dominated by fluorescence and intersystem crossing. This is known as Kasha's rule, with azulene as the textbook exception.[1] According to conventional wisdom, $S_1 \rightarrow S_0$ internal conversion is inefficient, with typical time constants in the nanosecond to microsecond range.[1,2] During the 1960s, Robinson and Frosch developed a theory that predicts a linear relationship between internal conversion rates and the Franck−Condon factor.[7,8] Supporting this idea, Siebrand established from experimental data on the $T_1 \rightarrow S_0$ transition for a series of hydrocarbons that the decrease in IC efficiency with increasing energy gap between the involved consecutive electronic states can be traced back to an exponential drop of the Franck−Condon factor with increasing vibrational quantum number.[9,10] The resulting linear dependence of the logarithm of the internal conversion rate versus the (electronic excitation) energy gap was theoretically corroborated[10,11] and is currently known as the well-established "energy gap law" for internal conversion.[1,2]

In recent years, several molecules have been found to exhibit considerably faster $S_1 \rightarrow S_0$ internal conversion than previously envisioned, reaching down into the femtosecond time regime,

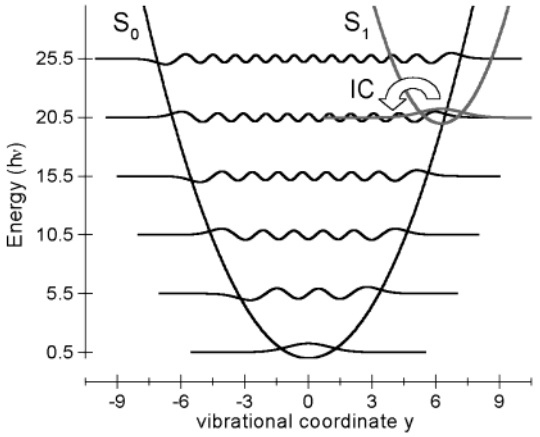

Figure 1. Schematic drawing of the internal conversion process, and illustration for calculations performed for Figure 6. Every fifth vibrational wave function is shown for the S_0 state. The situation in this picture results in maximal resonant Franck−Condon overlap for the displacement $D = \sqrt{39}$ (see text).

† Uppsala University.
‡ Max-Born-Institut für Nichtlineare Optik und Kurzzeitspektroskopie.

(1) Turro, N. J. *Modern Molecular Photochemistry*; University Science Books: Sausalito, CA, 1991.
(2) Michl, J.; Bonačić-Koutecký, V. *Electronic Aspects of Organic Photochemistry*; Wiley-Interscience: New York, 1990; Chapter 2.
(3) Klöpffer, W. *Adv. Photochem.* **1977**, *10*, 311.
(4) Cerullo, G.; Polli, D.; Lanzani, G.; De Silvestri, S.; Hashimoto, H.; Cogdell, R. J. *Science* **2002**, *298*, 2395.
(5) Pecourt, J.-M. L.; Peon, J.; Kohler, B. *J. Am. Chem. Soc.* **2001**, *123*, 10370.
(6) Blanchet, V.; Zgierski, M. Z.; Seideman, T.; Stolow, A. *Nature* **1999**, *401*, 52.
(7) Robinson, G. W.; Frosch, R. P. *J. Chem. Phys.* **1962**, *37*, 1962.
(8) Robinson, G. W.; Frosch, R. P. *J. Chem. Phys.* **1963**, *38*, 1187.
(9) Siebrand, W. *J. Chem. Phys.* **1966**, *44*, 4055.
(10) Siebrand, W. *J. Chem. Phys.* **1967**, *46*, 440.
(11) Siebrand, W. *J. Chem. Phys.* **1967**, *47*, 2411.

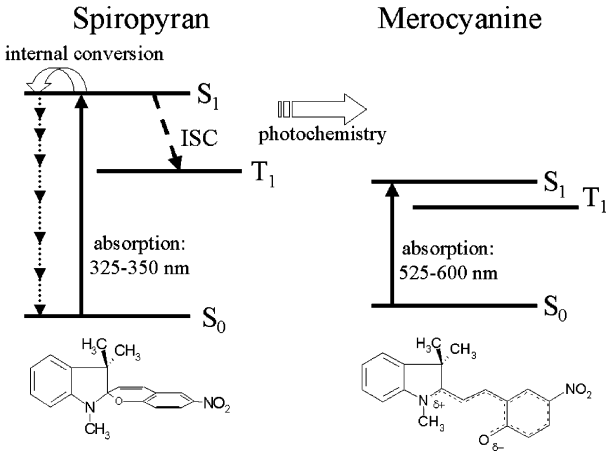

Figure 2. Photophysics and photochemistry of 6-nitro-BIPS.

such as DNA and RNA nucleosides.[5] Another interesting example is the green fluorescent protein (GFP) chromophore, a widely used biological marker for gene expression and protein localization in living organisms.[12,13] The fluorescence quantum yield of the GFP chromophore drops dramatically from 0.8 in the protein to almost nonfluorescent ($\sim 10^{-3}$) outside the protein environment,[13] due to rapid internal conversion. The current explanation of extremely rapid IC processes typically involves the concept of conical intersections.[14,15]

Recently, we started a time-resolved exploration of photochromic spiropyran-merocyanine molecular switches.[16,17] We observed that internal conversion and vibrational cooling back to the spiropyran ground state is a dominant fate for the spiropyran S_1 state.[16,17] This inspired us to investigate the influence that solvents have on the IC process. To this end, we studied the recovery of the vibrational absorption spectrum of the molecule 6-nitro-1′,3′,3′-trimethylspiro[2*H*-1-benzopyran-2,2′-indoline], further abbreviated as 6-nitro-BIPS, after excitation with UV light, in various solvents. The spiropyran compound is excited by 70 fs UV pulses ($\lambda \approx 325-330$ nm) to initiate the photophysical and photochemical processes (see Figure 2). Formation of merocyanine photoproducts and recovery of the spiropyran ground state was followed, at room temperature, by monitoring the time-evolution of the vibrational absorption spectrum in the fingerprint region with ~100 fs mid-IR pulses.[18] Optical pumping of spiropyran molecules from the electronic ground state (S_0) to the electronic excited state (S_1) results in an increased transmission (lower optical density) for the infrared probe pulse at vibrational frequencies of the spiropyran ground state. The time scale of the overall cooling process is reflected in the recovery kinetics of the transmission, and the $S_1 \rightarrow S_0$ IC quantum yields determine the final extent of the recovery.

Furthermore, we demonstrate, on the basis of an elementary theoretical analysis, that the physical mechanisms behind the energy gap law[7−11] can account for ultrafast internal conversion as well, but do not necessarily lead to the standard energy gap dependence.[1,2,10] In particular, we advance the idea that efficient $S_1 \rightarrow S_0$ internal conversion is related to large conformational changes upon optical excitation. This resembles conclusions of previous investigations, that identified the importance of structural rigidity in enhancing fluorescence quantum yields, and established promotion of internal conversion by flexible side-groups, known as "loose bolt" and "free rotor" effects.[1,19] As large conformational changes seem inherent to chemical reactions, fast internal conversion could be a rather common side-effect in many photochemical reactions. Our results also give further insight into the relevance of (conical) intersections for ultrafast internal conversion.

Experimental Section

Femtosecond UV pump/mid-infrared probe experiments were performed on 6-nitro-BIPS molecules in a number of solvents, selected to minimize solvent absorption in the investigated IR spectral range. The following solvents were used: tetrachloroethene (C_2Cl_4), chloroform ($CHCl_3$), *n*-hexane, and perdeuterated acetonitrile (CD_3CN), dimethyl sulfoxide ($(CD_3)_2SO$), and methanol (CD_3OD). The compound 6-nitro-BIPS and the solvents C_2Cl_4 and $CHCl_3$ were purchased from Sigma-Aldrich. The deuterated solvents (deuteration grade 99.8%) were purchased from Deutero GmbH. Steady-state emission spectra and excitation spectra were recorded on a SPEX Fluorolog2 system, using spectroscopic grade nondeuterated solvents purchased from Sigma-Aldrich.

The femtosecond pump−probe setup, based on a 1 kHz, 40 fs home-built amplified Ti:sapphire laser, has been described in detail previously.[18] The UV pump pulses for the electronic excitation are generated by sum frequency mixing of the Ti:sapphire fundamental and visible pulses coming from a noncollinear optical parametric amplifier. The pulse energy was 2−3 μJ, and the pulse duration was about 70 fs, as determined by self-diffraction autocorrelation. The probing mid-infrared pulses were generated by difference frequency mixing in a GaSe crystal of near-infrared signal and idler pulses coming from a double-pass collinear parametric amplifier pumped by the Ti:sapphire fundamental. Probe and reference pulses, derived using reflections from a BaF_2 wedge, were focused in the sample with a diameter of 150 μm and then dispersed in a grating spectrometer. Complete spectra were recorded for each shot using a nitrogen-cooled double HgCdTe detector array (2 × 32 elements). The delay zero and the time resolution (about 150 fs) were determined in a frequency-resolved cross-correlation measurement in a thin ZnSe crystal. The 6-nitro-BIPS molecule was dissolved in various solvents with a concentration of 0.01−0.02 M and pumped through a free streaming jet of nominal thickness 100 μm.

Results and Discussion

As a typical example of the absorption recovery kinetics of a spiropyran vibration, we show in Figure 3A the kinetics of the ~1340 cm^{-1} IR band, in $CHCl_3$ and $(CD_3)_2SO$. This IR absorption band is related to the symmetric stretching mode of the NO_2 substituent of 6-nitro-BIPS.[20] Identical behavior is observed for the ~1610 cm^{-1} vibration. The fraction of absorption recovery is taken as the IC quantum yield, ϕ_{IC}, which is found to vary from 34% in C_2Cl_4 to 80% in $(CD_3)_2SO$. Emission measurements (see below) demonstrate that the spiropyran triplet state is significantly populated only in C_2Cl_4. As a consequence, the spiropyran triplet state does not influence the dynamics in Figure 3A. Because the same kinetics is

(12) Tsien, R. Y. *Annu. Rev. Biochem.* **1998**, *67*, 509.
(13) Zimmer, M. *Chem. Rev.* **2002**, *102*, 759.
(14) Haas, Y.; Klessinger, M.; Zilberg, S. *Chem. Phys.* **2000**, *259*, 121, preface special issue on conical intersections.
(15) Kühl, A.; Domcke, W. *J. Chem. Phys.* **2002**, *16*, 263.
(16) Rini, M.; Holm, A.-K.; Nibbering, E. T. J.; Fidder, H. *J. Am. Chem. Soc.* **2003**, *125*, 3028.
(17) Holm, A.-K.; Rini, M.; Nibbering, E. T. J.; Fidder, H. *Chem. Phys. Lett.* **2003**, *376*, 214.
(18) Rini, M.; Kummrow, A.; Dreyer, J.; Nibbering, E. T. J.; Elsaesser, T. *Faraday Discuss.* **2003**, *122*, 27.
(19) Lewis, G. N.; Calvin, M. *Chem. Rev.* **1939**, *25*, 273.
(20) Schiele, C.; Arnold, G. *Tetrahedron Lett.* **1967**, *13*, 1191.

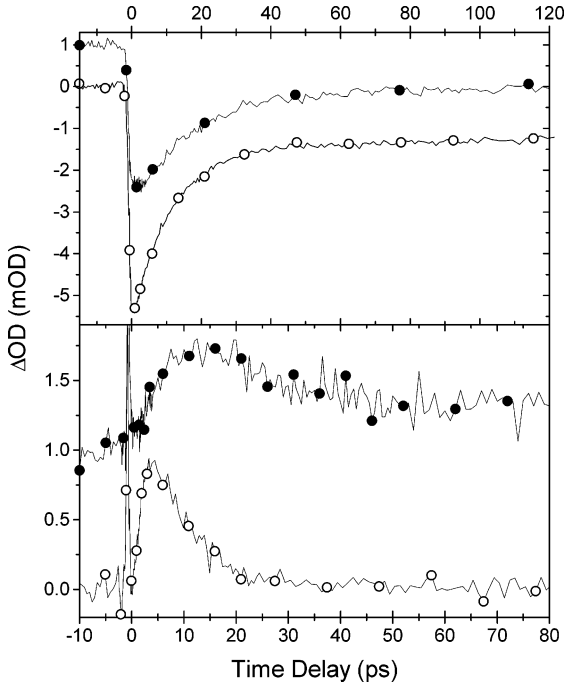

Figure 3. (A) Absorption recovery kinetics at the ~1340 cm^{-1} IR band of 6-nitro-BIPS in $CHCl_3$ (−●−) and $(CD_3)_2SO$ (−○−). (B) Transient kinetics related to vibrational cooling in $CHCl_3$ (−●−) and $(CD_3)_2SO$ (−○−) at ~1320 cm^{-1}. Signals in $CHCl_3$ are raised by 1 mOD for representation purposes.

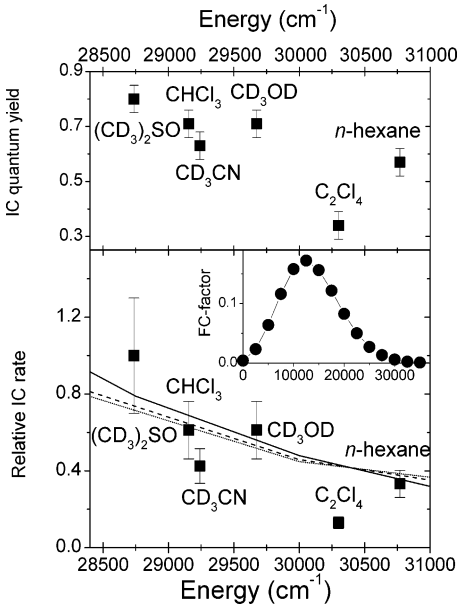

Figure 4. (A) Internal conversion quantum yield (■) versus the position of the spiropyran $S_0 \rightarrow S_1$ absorption maximum in various solvents. (B) Relative IC rates (■) derived from the data in (A) using eq 1. The lines illustrate the behavior of the Franck−Condon factor for transitions $v' = 0 \rightarrow v = n$, for three vibrational energies. These energies $h\nu$ and the corresponding displacements D are as follows: $h\nu = 1250$ cm^{-1}, $D = 5.4$ (—); $h\nu = 2500$ cm^{-1}, $D = 3.3$ (- -); and $h\nu = 3750$ cm^{-1}, $D = 2.4$ (·····). The inset illustrates for the second combination the expected behavior over a larger energy gap range.

observed at different bleached spiropyran vibrational absorption bands, we can exclude that the kinetics is related to coincidental overlap with vibrational bands of the merocyanine isomers. In addition, merocyanine product formation (not shown), determined at ~1415 cm^{-1} where the spiropyran has no IR band, occurs with different time constants. The data in Figure 3A lead to vibrational cooling time constants, after internal conversion, of 23 ps in $CHCl_3$, and 11 ps in $(CD_3)_2SO$. The merocyanine product formation time constants are 14 ps in $CHCl_3$, and 15 ps in $(CD_3)_2SO$, respectively. Nitro-groups are known to enhance internal conversion through the "loose bolt" effect.[19] We stress that in the present case the ultrafast internal conversion is not related to the nitro-group, as a previous investigation[16] by us on the related compound BIPS (6-nitro-BIPS without the nitro-group) in C_2Cl_4 also demonstrated ultrafast IC for this compound, with an even higher IC quantum yield of ~90%. In Figure 4A, the IC data for 6-nitro-BIPS are plotted against the $S_1 \rightarrow S_0$ energy gap.

Increased absorption is also observed at various frequencies. Such signals arise from excited-state intermediates, photoproducts, or vibrationally hot spiropyran molecules in the S_0 electronic state. In Figure 3B, we show increased transient absorption at ~1320 cm^{-1}. These transient signals are also related to the NO_2 symmetric stretching mode, but are red-shifted due to anharmonicity. Two effects cause the red-shift: (1) The intrinsic anharmonicity of a vibrational ladder results in increasingly smaller transition energies from higher vibrational quantum levels. (2) Couplings to other vibrational modes introduce additional anharmonicities, and as a result the $v = 0 \rightarrow v = 1$ transition energy of a mode changes if other vibrational modes become highly excited.[18] Consequently, the data in Figure 3B do not automatically imply that the vibrational relaxation occurs (exclusively) through the ~1340 cm^{-1} mode. However, the rise times of the signals in Figure 3B do provide an upper limit to the IC time constant, which is 3.6 ps in $(CD_3)_2SO$ and 6.4 ps in $CHCl_3$.

The IC quantum yield, ϕ_{IC}, apparently increases very modestly with decreasing energy gap (Figure 4A). In our case, the energy gap (more precisely: the $S_1 \rightarrow S_0$ absorption maximum) of a single molecular species is modified by solvent−solute interactions, while Siebrand analyzed data where variation of the energy gap was obtained by comparing a series of related different molecular species.[7−9] Figures 3 and 4 illustrate two aspects that are not within the conventional understanding of the energy gap law:[2,3] extremely efficient internal conversion can take place (1) on picosecond or even subpicosecond time scales, and (2) even at rather large energy gaps where Franck−Condon factors are thought to be very small.

Relative internal conversion rates, k_{IC}^{rel}, are calculated from the ϕ_{IC} data in Figure 4A using the equation

$$k_{IC}^{rel} \propto \phi_{IC}/(1 - \phi_{IC}) \qquad (1)$$

This equation assumes that it is predominantly the internal conversion rate that is affected by the change in energy gap with solvent. Figure 4B shows a plot of k_{IC}^{rel} versus the energy gap. The variation of k_{IC}^{rel} with energy gap is still modest, although somewhat stronger than that for the IC quantum yield. In support of the above-mentioned assumption underlying eq 1, we point out the following: If the drop in ϕ_{IC} with increasing energy gap instead stems from an enhancement of either the intersystem crossing rate or the rate of the photochemistry, the responsible process would actually exhibit a trend opposite to that of the energy gap law. Recall that experimental verification of the energy gap law was in fact performed on data related to an intersystem crossing transition: $T_1 \rightarrow S_0$. In addition, we

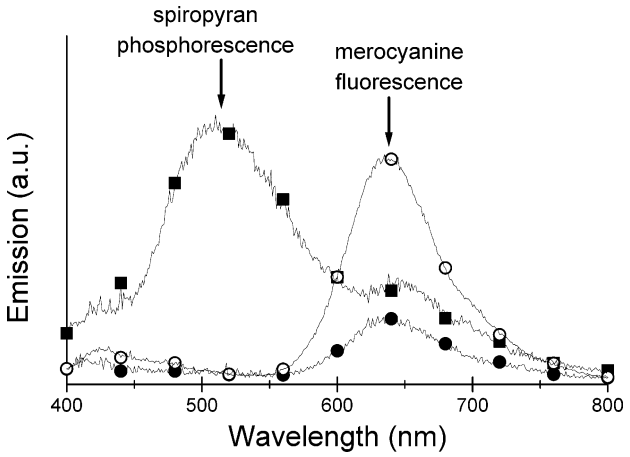

Figure 5. Emission spectra after excitation at 330 nm for 6-nitro-BIPS in C_2Cl_4 (−■−), CH_3CN (−●−), and CH_3OH (−○−).

mention that the combination of higher IC quantum yield and a faster vibrational hot band rise time in $(CD_3)_2SO$ as compared to $CHCl_3$, as illustrated in Figures 4A and 3B, confirms the conclusion that the higher IC quantum yield is caused by an increase in internal conversion rate.

Only the data point for the solvent C_2Cl_4 deviates significantly from the general trend in Figure 4. We investigated the emission properties of 6-nitro-BIPS in all solvents. While at 77 K we detected spiropyran phosphorescence in all solvents, with peaks at ∼471 and ∼508 nm, we observed at room temperature phosphorescence only in C_2Cl_4,[21] now broadened and peaking around 510 nm. Room-temperature emission spectra after excitation at 330 nm of 6-nitro-BIPS in some of the solvents are shown in Figure 5. The deviation of C_2Cl_4 from the observed trend is therefore most likely the result of a much more efficient intersystem crossing in this solvent. In the other solvents, intersystem crossing seems to be a negligible channel. The increased intersystem crossing yield in C_2Cl_4 cannot be attributed to a heavy atom effect, as no phosphorescence is detected in $CHCl_3$. All spectra show also merocyanine emission around 650 nm, related to excitation of the tiny fraction of the molecules which is present in this form. Emission excitation spectra (not shown) confirm that the 510 nm band in C_2Cl_4 is related to excitation of the first electronic absorption band of the spiropyran, whereas the ∼650 nm fluorescence band is related to excitation of the merocyanine.

The clue to understanding the weak energy gap dependence and high IC efficiency is found by examining the effect of changes in equilibrium conformation (coordinate) upon optical excitation. A simple illustrative model situation is sketched in Figure 1. We assume harmonic oscillator potential energy surfaces (PES), and the effect of conformation changes is approximated by introducing a displacement along a single distorting vibrational mode. In Figure 1, the displacement D is $\sqrt{39}$ (∼6.2) in units of the vibrational coordinate $y = (k/h\nu)^{1/2}x$, where k is the vibrational force constant and ν is the vibrational frequency. Our displacement parameter D is linear in the vibrational coordinate and is related to Siebrand's displacement parameter[10] γ by $\gamma = {}^1/_2y^2$. The harmonic potential energy function $V = {}^1/_2kx^2$ becomes $V = {}^1/_2h\nu y^2$, upon substitution of x by y. In Figure 1, the excited-state PES is elevated by 20

(21) See also: Reeves, D. A.; Wilkinson, F. *J. Chem. Soc., Faraday Trans. 2* **1973**, *69*, 1381.

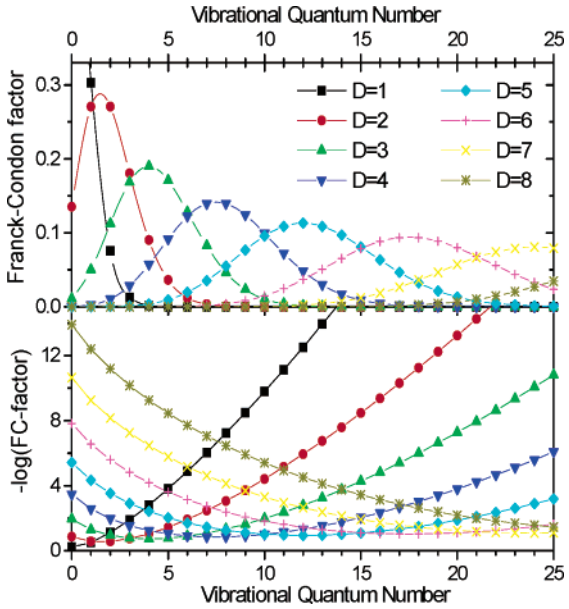

Figure 6. (A) Franck−Condon factor for transitions between the excited-state $\upsilon' = 0$ vibrational wave function and ground-state vibrational wave functions, for the vibrational quantum number $\upsilon = 0-25$, and for displacements $D = 1-8$. (B) Logarithmic plot of the Franck−Condon factor (multiplied by −1), to facilitate comparison to the "energy gap law" prediction.

vibrational quanta, which for the energy gaps observed for 6-nitro-BIPS would correspond to a vibrational ladder with vibrational quanta of about 1250 cm^{-1}. In Figure 6A, we illustrate how the Franck−Condon factor of the excited-state $\upsilon' = 0$ vibrational wave function with the ground-state vibrational wave functions changes with vibrational quantum number and increasing displacement of the excited-state PES. The main features to be noted are as follows: (1) The Franck−Condon factor peaks at increasingly higher vibrational quantum numbers with increasing displacement. (2) Sizable Franck−Condon factors are obtained over increasingly larger ranges of this quantum number for larger displacements.

Figure 6B plots the same data in the manner done by Siebrand[10] for displacements $D = 1, \sqrt{2}, 2$, and for $\upsilon = 0-7$. For $D = 1-5$, Figure 6B illustrates at higher values of υ the type of behavior expected according to the energy gap law. Note that the slope decreases for higher values of D. Plots for higher values than $D = 2$ are not found in the literature. Figure 6B also demonstrates that for higher values of D the behavior (depicted here up to $\upsilon = 25$) can even become more or less opposite to the traditional energy gap law prediction. Consequently, these calculations indicate that the energy gap law is not valid for transitions between electronic states for which the molecule has a very different structure.

Now, we demonstrate that the data in Figure 6 can account for the observed weak energy gap dependence. The lines in Figure 4B illustrate that many combinations of vibrational energy and displacement are in accordance with the observed trend. These lines are linear interpolations of consecutive Franck−Condon factors for the following combinations: $h\nu = 1250$ cm^{-1}, $D = 5.4$ (—); $h\nu = 2500$ cm^{-1}, $D = 3.3$ (- -); and $h\nu = 3750$ cm^{-1}, $D = 2.4$ (•••••). The inset depicts the trend of the FC-factor over a wider energy range for the combination $h\nu = 2500$ cm^{-1} and $D = 3.3$. The trend established by these fits indicates that fitting the data with displacements smaller

than about 2.4 calls for unrealistic vibrational frequencies, as typically vibrational frequencies do not exceed 4000 cm^{-1}. To quantify the weak energy gap dependence, we have examined the derivative of plots as in Figure 6B for the combinations of displacement and vibrational energy that fitted the data in Figure 4B. For both $D = 2.4$ and $D = 3.3$, the first derivative of the logarithmic plots appears to be about 2.1 times higher at $v = 24.5$ than in the energy range covering our experimental data. Plots of the first derivative further indicate that for both $D = 2.4$ and $D = 3.3$, true energy gap law behavior, exemplified by a constant value for the derivative, has not been reached yet at $v = 25$. In the case of the fit with $D = 5.4$, the experimental data fall in the high end of our calculated range: $v = 23-25$.

Experimental information on the displacement is in principle attainable from the intensity pattern of the vibronic progression in the absorption spectrum. However, large displacements are expected if the excited-state structure of the molecule differs significantly from the electronic ground-state structure. The excited-state PES will then not only be displaced, but also have a different shape (and associated force constant k). As a consequence, the vibronic structure of the progression $v = 0 \rightarrow v'$ will in practice not be representative for that of $v \leftarrow v' = 0$.[22] Another complication is that inhomogeneous and lifetime broadening (due to ultrafast IC) often results in very little discernible vibronic structure in absorption spectra of these molecules, as is the case for 6-nitro-BIPS. On the other hand, low-temperature spectra of merocyanine isomers of spiropyrans do have clear vibronic progressions in nonpolar media. On the basis of such spectra, we derive for the merocyanine of BIPS at 10 K in argon[23] a displacement $D = 1.9$, and for the merocyanine of 6-nitro-BIPS in methylcyclohexane at 77 K $D = 1.5$. These numbers suggest that certainly displacements of about $D = 2-3$, as encountered in fitting the data in Figure 4B, are not beyond reason.

The concept of large conformational changes upon optical excitation, forwarded here, even provides a further rationale to the relevance of conical intersections for ultrafast internal conversion.[14,15] Analysis of the data in Figure 6A reveals the following relation between the vibrational quantum number with maximum Franck−Condon factor and the displacement:

$$v_{\mathrm{FCmax}} = {}^1/_2(D^2 - 1) \qquad D \geq 1$$

and

$$v_{\mathrm{FCmax}} = 0 \qquad D \leq 1$$

The condition of energy conservation during the actual internal conversion process then requires that the excited-state PES is raised above the ground-state PES by $h\nu v_{\mathrm{FCmax}}$. Graphically, this always corresponds to a situation as depicted in Figure 1, where the ground-state PES exactly crosses through the bottom of the excited-state PES. Coupling of PESs at crossings can lead to conical intersections.[24] Our result indicates that internal conversion from $v' = 0$ will be most efficient at such intersections[25] and thereby unites perturbation theory-based approaches and quantum theoretical calculation methods. Note that IC from levels other than $v' = 0$ could present an additional source for deviations from standard energy gap law behavior.[25] Initially, the electronic energy should predominantly be converted into vibrational energy of those vibrational coordinates along which such (conical) intersections occur. This opens up the possibility of identifying the modes most active in the internal conversion process by performing picosecond time-resolved resonance Raman scattering experiments.[26] Quantum theoretical modeling of ultrafast IC aimed at identifying a coupling mode and tuning modes[15] is therefore supported by our analysis.

Finally, one may wonder if the results in Figure 4 justify pico- and femtosecond time scales for internal conversion processes. For this, we return to Siebrand and Williams' work[9−11,27] on $T_1 \rightarrow S_0$ and $S_1 \rightarrow S_0$ internal conversion in hydrocarbons. They introduced the parameter $\alpha(E_0)$,[11,27] which can be interpreted as the maximum IC rate that is reached for a Franck−Condon factor of 1. Their analysis on hydrocarbons[27] led to a value $\alpha(E_0) \approx 10^{13}-10^{14}$ s^{-1}. The FC-factors at 30 000 cm^{-1} for the plots in Figure 4B are 0.0066 ($D = 2.4$), 0.0061 ($D = 3.3$), and 0.0064 ($D = 5.4$). Although the value of $\alpha(E_0)$ may not be a universal constant for all types of molecules, combining these two pieces of information indicates that for the spiropyran molecule IC time constants in the order of 1−10 ps are fully in line with expectations. Clearly, large conformational differences between the excited and the ground state can explain ultrafast IC, within the theoretical framework of the "energy gap law". On the other hand, we predict that these molecules will typically not exhibit the standard energy gap law behavior.

Our findings have important implications for many chemical processes, as chemical reactions by definition involve conformational and structural changes. For instance, it opens interesting avenues in the design of efficient photochromic switches. Depending on the exact conformational changes that accompany different electronic transitions, a tradeoff could be achieved between ultrafast IC and rapid "internal" conversion to photoproducts. This is illustrated by efficient subpicoseond photoproduct formation in the dihydroazulene/vinylheptafulvene photochromic switch, which has been ascribed to a conical intersection of the reactant excited electronic state and the photoproduct electronic ground state.[28] Enhancing photochemistry quantum yields over IC, or vice versa, could also be an important function of protein structures in biochemistry. As a prime example, we mention the GFP system.[12,13,29] Quantum mechanical calculations led to the conclusion that the two halves of the free GFP chomophore are planar in the S_0 electronic state, while they are perpendicular in the S_1 state.[29] The high fluorescence quantum yield of the GFP chromophore in the

(22) So-called "mirror symmetry" of absorption and fluorescence requires the same force constant for excited- and ground-state PESs, as well as symmetrical PESs around the coordinate y_0 where V is minimum, that is: $V(y_0 - y) = V(y_0 + y)$.

(23) Ernsting, N. P.; Arthen-Engeland, T. *J. Phys. Chem.* **1991**, *95*, 5502.
(24) Yarkony, D. R. *Acc. Chem. Res.* **1998**, *31*, 511. This paper points out that for molecules of three atoms or more, even states of the same symmetry are permitted to intersect, instead of resulting in an avoided crossing ("noncrossing rule").
(25) Reference 14 mentions the question whether IC takes place at the absolute minimum of the PES or also at other "points" as an important issue in research on conical intersections.
(26) Kozich, V.; Werncke, W.; Vodchits, A. I.; Dreyer, J. *J. Chem. Phys.* **2003**, *118*, 1808.
(27) Siebrand, W.; Williams, D. F. *J. Chem. Phys.* **1968**, *49*, 1860.
(28) Boggio-Pasqua, M.; Bearpark, M. J.; Hunt, P. A.; Robb, M. A. *J. Am. Chem. Soc.* **2002**, *124*, 1456.
(29) Voityuk, A. A.; Michel-Beyerle, M.-E.; Rösch, N. *Chem. Phys. Lett.* **1998**, *296*, 269.

protein has been suggested to originate from blocking this conformational change, thereby allowing proton transfer to take place from the excited chromophore to an extensive hydrogen-bonding network formed by the protein binding pocket.[29] Controlling chemical conformations by rigid matrices or protein environments could therefore be an important aspect in nature's way to alter the efficiency of (photo)chemical events.

Acknowledgment. This work benefited from financial support by the Swedish Research Council (Vetenskapsrådet), the Deutsche Forschungsgemeinschaft (Project DFG NI 492/2-2), and financial travel support by the LIMANS Cluster of Large Scale Laser Facilities (Project Nr. MBI000237).

JA038741Y